Volume 10, Issue 1, June 2023 ISSN 2542-2545

The HIMALAYAN PHYSICS

A peer-reviewed Journal of Physics

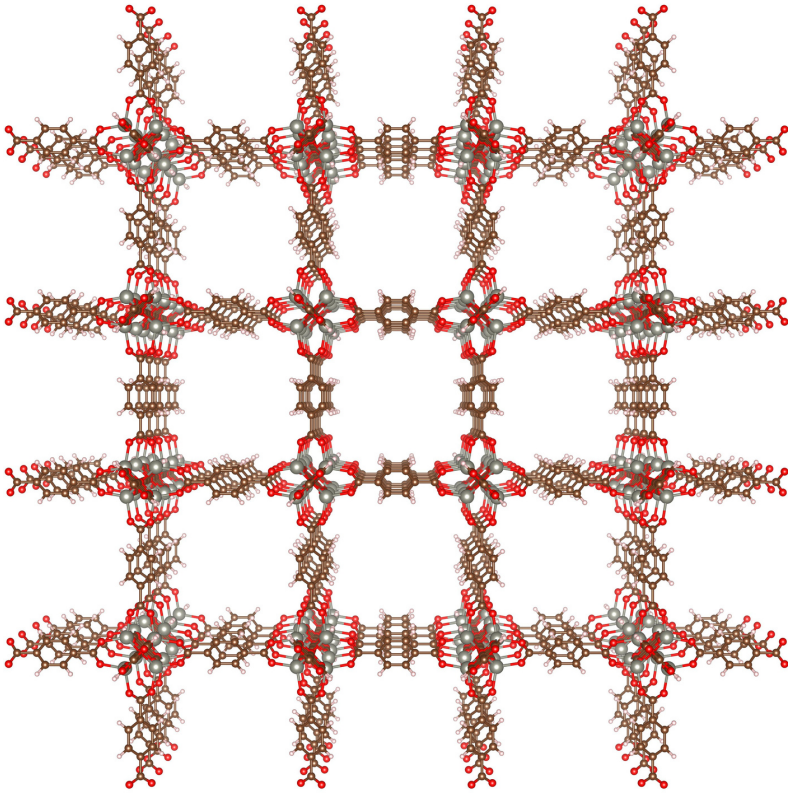

Department of Physics, Prithvi Narayan Campus, Pokhara
Nepal Physical Society, Gandaki Chapter, Pokhara

Publisher

Department of Physics, Prithvinarayan Campus, Pokhara
Nepal Physical Society, Gandaki Chapter, Pokhara

The Himalayan Physics

Volume 10, Issue 1, June 2023

ISSN 2542-2545

The Himalayan Physics (HimPhys) is an open access peer-reviewed journal that publishes quality articles which make innovative contributions in all areas of Physics. HimPhys is published annually by Nepal Physical Society (Gandaki Chapter), and Department of Physics, Prithvi Narayan Campus, Pokhara. The goal of this journal is to bring together researchers and practitioners from academia in Nepal and abroad to focus on advanced techniques and explore new avenues in all areas of physical sciences and establishing new collaborations with physics community in Nepal.

Chief Editor

Aabiskar Bhusal

©2023, Publishers. All rights reserved.

This publication is in copyright. Subject to statutory exception and to the provisions of relevant collective licensing agreements, no reproduction of any part may take place without written permission of the publishers.

Cover: Ball-and-stick model of MOF-5. © Roshani Sharma. Printed with permission.

Volume 10, Issue 1, June 2023 ISSN 2542-2545

The HIMALAYAN PHYSICS

A peer-reviewed Journal of Physics

Chief Editor

Aabiskar Bhusal

Publisher

Department of Physics, Prithvi Narayan Campus, Pokhara
Nepal Physical Society, Gandaki Chapter, Pokhara

Nepal Physical Society

Gandaki Chapter

Pokhara, Nepal

President
Dr. Krishna Raj Adhikari

Immediate Past President
Min Raj Lamsal

Vice-President
Dr. Kapil Adhikari

Secretary
Ravi Karki

Treasurer
Dipak Adhikari

Joint Secretary
Amrit Dhakal

Editorial Member
Aabiskar Bhusal

Members
Bhuban Subedi
Man Bahadur Roka
Sabin Gautam
Sristi Gurung
Suresh Poudel

Advisory Board
Pabitra Mani Poudyal
Surya Bahadur G.C.
Parashu Ram Poudel
Jeevan Regmi
Kul Prasad Dahal

Himalayan Physics Vol-10(1) (2023)

TABLE OF CONTENTS

Adsorption of toxic gases by metal-organic frameworks
D. Adhikari, R. Karki, K. Adhikari, N. Pantha 1

Cluster modelling of MOF-5 and its application on gas storage
R. Sharma, S. Gurung, K. Adhikari 25

Electronic and magnetic properties of ternary sulfide $Rb_2Mn_3S_4$
G.B. Acharya, M.P. Ghimire 33

Dust properties around NGC 7023 nebula in interstellar medium using IRIS, AKARI, and WISE survery
A. Subedi, A. Chaudhary, K. Chaudhary, K. Khatiwada, R. Kandel, S. N. Yadav, D. R. Upadhyay, A. K. Jha 40

Experimental design for tri-state logic
H.S. Mallik, R. Rijal, H.P. Lamichhane 51

Comparison of aerosol optical properties over Lumbini, Pokhara and Langtang-Base Camp
S. Sapkota, S. Gautam, A. Gautam, R. Poudel, S. Pokheral, K. Basnet, A. Subedi 58

Wavelet coherence analysis foF2 over Boulder station during different geomagnetic activity
A. Giri, B. Adhikari, B. Shrestha, S. Rimal 66

Complex impedance analysis of soft chemical synthesized NZCF systems
D. Parajuli, V.K. Vagolu, K. Chandramoli, N. Murali, B.R. Sharma, N.L. Shah, K. Samatha 78

Controlling pests in post-harvested wheat using microwave heating
H.B. Pariyar, S. Dhungana, D.R. Paudel 86

Mean value and velocity variation of ions in different magnetic field at constant obliqueness
B.R. Adhikari 99

Comparative study of solar flux using different empirical models at low land urban industrial zone of Biratnagar Nepal
F. Limbu, B.R. Tiwari, U. Joshi, J. Regmi, I.B. Karki, K.N. Poudyal 100

****

Him. Phys. **10(1)** 58-65, (2023)

Himalayan Physics

Comparison of aerosol optical properties over Lumbini, Pokhara and Langtang-Base Camp

Research Article

Santosh Sapkota[1], Sabin Gautam[1,2*], Aayush Gautam[3], Resham Poudel[1], Santosh Pokheral[1], Kailash Basent[1], Aabiskar Subedi[1]

1 Prithvi Narayan Campus, Tribhuvan University

2 Pokhara Astronomical Society (PAS)

3 Birendra Multiple Campus, Tribhuvan University

Abstract: The comparative study of aerosol optical properties at different tourist places in Nepal has been performed. Lumbini, Pokhara and Langtang-Base Camp (BC) were the places chosen for observation. Aerosols are made up of a variety of airborne particles both fine and coarse and are most prevalent in urban industrial Areas. The data was collected from AERONET websites between 2017 and 2019 for each of the locations. The ranges of AOD over Pokhara and Langtang-BC were discovered to be lower (0.1 and 0.01) and the maximum and minimum values of AOD (675 nm) in Lumbini occurred predominantly in winter and summer monsoon respectively. The causes of the highest AOD levels were land clearing for crop cultivation and vegetation fires which were then followed by biomass burning for heating purposes and pollution from brick kilns, industry and vehicles. AOD, angstrom exponent (α and β) and Visibility are distinct from typical seasonal variations. The total AE fluctuations show that a combination of fine and coarse mode particles as well as anthropogenic aerosols made up the majority of the aerosol loading during the research period. Visibility was inversely related to the turbidity coefficient (β). Three times as much visibility was discovered over Langtang-BC as compared to Lumbini and Pokhara. Over these three locations, precipitable water peaked in the summer and dropped in the winter. These three sites seasonal changes are found to be distinct for each parameter.

Keywords: Aerosol optical depth (AOD) • Angstrom exponent (α) • Turbidity Coefficient (β) • Visibility

I. Introduction

Aerosols are mixtures of solid or liquid particles that combine with gas to generate a mixture whose features are mostly unknowable and play a significant influence in predicting the global climate. Anthropogenic factors (burning fossil fuels, biomass, transportation, etc.) or natural factors can both produce aerosols (volcanic, sea salt, desert, etc.). Aerosols range in size and shape from a few macromolecules to 100 μm, but depending on the level of pollution, they can reach a size of 10,000 microns.

Despite having significant uncertainties, Aerosol is one of the key variables in today's projection of global climate change. Studying atmospheric physics is important for understanding phenomena like precipitation and

* *Corresponding Author: sabin.gtmk3k@gmail.com*

the radiative transport of light waves in the atmosphere [1]. Complex aerosol optical and microphysical properties over a wide range of both temporal and spatial scales are major reasons why scientific understanding of aerosols is still limited. Aerosols have the potential of absorbing and scattering solar energy which ultimately influences the climate system of the earth [2]. Aerosols loading in the atmosphere has a major effect on the climate system, reducing visibility and crop productivity, and deteriorating human health mainly related respiratory system due to sub-micron aerosols [3, 4]. The major challenge in the current climatic study is to characterize the variation of concentration, composition and size of aerosols at regional scale with sufficiently high temporal and spatial resolution [5] Anthropogenic emissions from industry, transport and incomplete fossil fuel combustion are rapidly rising in China and India [6] which are known as Indo-Gangetic Plains (IGP). Lumbini also lies in the IGP region and is also affected by pollution [7]. Because of their large populations, closeness to the IGP region [8] and anthropogenic activities like burning biomass during the winter and burning fossil fuels. Lumbini and Pokhara experience higher aerosol loading Whereas in Langtang aerosol loading is due to the burning of biomass (e.g., cow dung, wood, fuel) to cook food [4]. The Himalaya Mountain located along the southern edge of the Tibetan plateau (TP) acts as a natural barrier for the transport of atmospheric aerosols [8]. Our data span three years from 2017 to 2019 and were taken from the AERONET website at 2.0 version. AERONET is a network of ground-based Sun photometers that measure atmospheric aerosol properties which are installed in around 400 stations all around the globe [9]. AERONET has also deployed a device that monitors aerosol loading at various wavelengths. Parameters such as Aerosol Optical Depth (AOD), Angstrom Exponent (α), Turbidity Coefficient (β), Precipitable Water (PW) and visibility have been studied in this paper. The Turbidity Coefficient (β) reflects the amount of aerosol rich in the given location whereas the Angstrom exponent (α) denotes aerosol size distribution. The amount of solar radiation absorbed about the amount of solar energy transmitted is known as the aerosol optical depth (AOD). The spectral variation of AOD which can be characterized by Angstrom's parameters gives an idea of particle size and aerosol loading in the atmosphere [10] additionally it provides a figure for the amount of direct sunlight that aerosol particles block from reaching the earth's surface [11]. The amount of precipitation on the earth's surface when the cloud condenses is known as precipitable water (PW). It is also one of the main components of a greenhouse because it is capable of absorbing and re-emitting infrared radiation. Visibility is affected by the physical and chemical properties of the particulate matter and the ambient relative humidity (RH). An increase in atmospheric particulate pollution results in a decrease in visibility [12–14]. This work mainly focuses on the understanding of AOD behavior concerning wavelength and the relation between the Angstrom exponent, precipitable water, and the Visibility of different stations over Nepal.

II. Data Set and Methodology

AERONET websites provided three levels of data as level 1.0 (unscreened), level 1.5 (cloud screened), and level 2.0 (quality-assured data). The data for Lumbini, Pokhara and Langtang-BC were collected at level 2.0 from

January 2017 to December 2019. The aerosol Robotic Network is a ground-based network of standardized camel sun sensors that measure AOD from 340nm to 1640nm and other parameters. For over a decade, AERONET has been providing high-quality retrievals of aerosol optical characteristics from the surface at global locations. Seasons in the South Asia region are divided into four categories: Winter (December to February), Pre-monsoon (March to May) Summer (June to September) and Post-Monsoon (October to November). The Table 1 gives the details about the selected region for our study.

Table 1. Details about the study area

Sites	Site Coordinates	Site Description
Lumbini	Latitude: 27.49000° North Longitude: 83.28000° East Elevation: 110.0 m	The location lies in Nepal's Southern Plain, which is part of the Indo-Gangetic plain
Pokhara	Latitude: 28.18664° North East Longitude: 83.97518° Elevation: 800.0 m	ALA The instrument can be found on the roof of the Shangrila Village resort on the outskirts of Pokhara, Nepal
Langtang BC	Latitude: 28.21443° North Longitude: 85.60978° East Elevation: 4901.0 m	The instrument is positioned in the enclosed area of the ICMOD met station in Langtang valley, near the Yala glacier

The relationship between AOD and angstrom exponent (α) is given by the power-law equation [15],

$$\tau = \beta\lambda^{-\alpha} \tag{1}$$

The wavelength in microns associated with AOD values is denoted by λ. Angstrom's turbidity coefficient is denoted by β. Equation (1) can be written in the logarithmic format as:

$$ln\tau(\lambda) = ln\beta - \alpha ln\lambda \tag{2}$$

Ångström parameters α and β were obtained from equation (2). From the spectral AOD(λ), the angström exponent α can be further defined as:

$$\alpha = -\frac{dln\tau AOD(\lambda)}{dln\lambda} = -\frac{ln\left(\frac{\tau AOD\lambda_2}{\tau AOD\lambda_1}\right)}{ln(\frac{\lambda_2}{\lambda_1})} \tag{3}$$

The visibility (V) of the air in km is given by the following formula [16]

$$\beta = 0.5\alpha\left(\frac{3.912}{V} - 0.01162\right) \times [0.02472(V-5) + 1.132] \tag{4}$$

Where V denotes the visibility in the atmosphere which is inversely proportional to the extinction coefficient [17].

III. Results and Discussion

Monthly and seasonal variation of aerosol optical properties

We addressed the average value of the monthly and seasonal fluctuations of AOD, Angstrom exponent (AE), Visibility, and Precipitable Water over three tourism stations in Nepal. The monthly mean AOD (675 nm) in Langtang BC, Lumbini, and Pokhara From 2017 to 2019 (Fig. 1). The monthly means are computed using daily averaged data and averaged across three years.

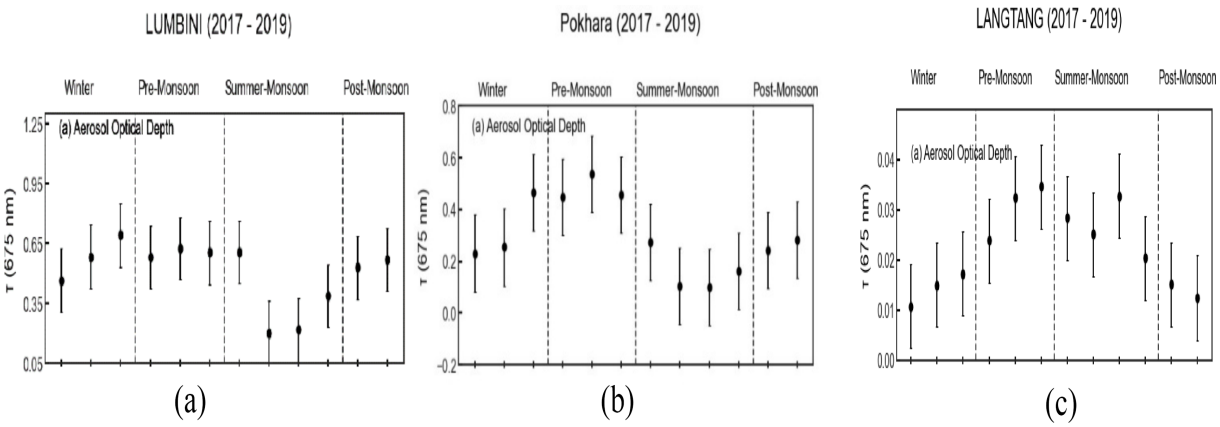

Figure 1. Demonstrates that the monthly mean AOD in (a) Lumbini, (b) Pokhara, and (c) Langtang BC peaks throughout the pre-monsoon

AOD above Lumbini is greatest in the winter (0.70) and pre-monsoon seasons (0.65). Winter haze in places like Pokhara and Lumbini is caused by an increase in heating needs, vehicle traffic, and industry. The highest and lowest values of AOD have been found over Pokhara, with the highest in pre-monsoon (0.45) and the lowest in monsoon (0.10). Pokhara is also located in an area of Nepal where there is a substantial amount of biomass burning and the proximity of the Indo-Gangetic plains contributes to haze throughout the winter and pre-monsoon seasons. During the study period, the monsoon season (0.25) had the lowest AOD value over Lumbini and Pokhara. The dramatic decrease in the AOD value during July is caused by the washout of aerosols caused by strong monsoon precipitation. As a result of this, AOD at Pokhara and Lumbini were significantly greater than at Langtang each month [8].

However, the AOD value in Langtang BC is lower than in Pokhara and Lumbini. The value was highest during the pre-monsoon season (0.03) and lowest during the post-monsoon season (0.01). The high Himalayas are dominated by higher concentrations during the winter and pre-monsoon, lower concentrations during the post-monsoon season, and rising levels during the winter to pre-monsoon. The value of AOD is greater than 0.02 during the pre-monsoon and monsoon seasons and less than 0.02 during the post-monsoon and pre-monsoon seasons. The accumulation of high-speed dust particles may be responsible for the rising value of AOD during the pre-monsoon season. The lower winter levels are attributed to a reduction in larger particles. The presence

of anthropogenic sources at Himalayan sites is responsible for the high AOD in pre-monsoon when the carried dust is at its peak. Monsoon begins with sporadic showers and pollution has contributed to monsoon haze, fog, and so on. Most residents in Langtang rely on biomass burning, a traditional fuel source that emits massive volumes of aerosol into our environment. AOD was observed to be increasing in the pre-monsoon season because the pre-monsoon season begins with low rain, making days hazy and land clearing adds significantly more aerosol to those hazy days. Because of the wet days of summer, AOD was found to be diminishing in Post-Monsoon and Post-Monsoon begins with the end of the monsoon when the sky is seen clearly with significantly less aerosol.

Monthly and seasonal variation of Angstrom Exponent (AE) and Visibility

Monthly means of Angstrom exponent (α (440-870 nm), Turbidity Coefficient (β), precipitable water (PW), and Visibility estimated from multiyear monitoring at AERONET locations in Lumbini, Pokhara, and Langtang-BC Nepal from 2017 to 2019 respectively are shown in Fig. 2.

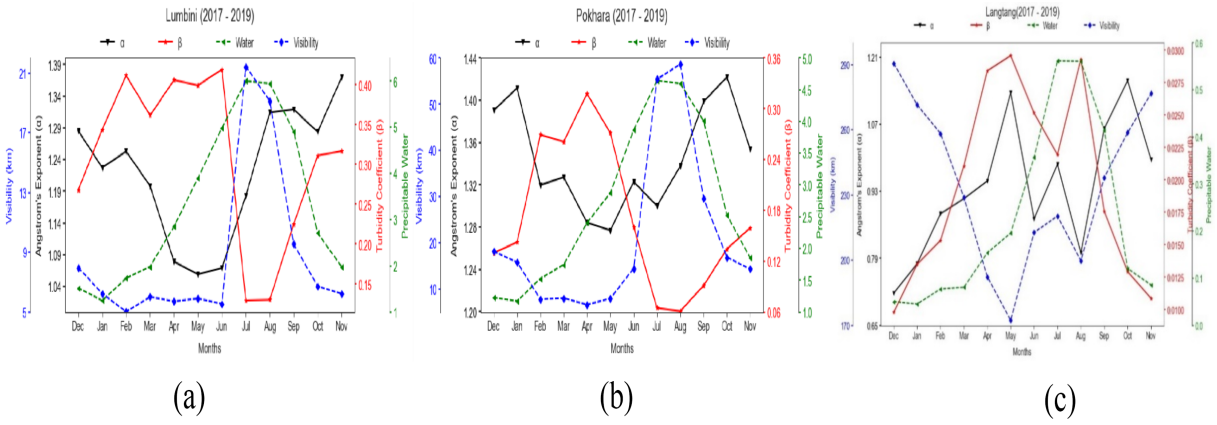

Figure 2. Comparison Angstrom exponent (α), Turbidity Coefficient (β), precipitable water (PW), and Visibility over Lumbini, Pokhara, and Langtang-BC.

The turbidity coefficient (β) represents aerosol loading, while the Angstrom exponent (α) represents aerosol size. The value of (α) ranges from 0.66 to 1.5 indicating that several forms of aerosols exist in the atmosphere over Lumbini, Pokhara, and Langtang BC. At Lumbini (Fig. 2), the Angstrom Exponent has a maximum value in the winter and post-monsoon months (November and December) exceeding 1.24 and a minimum value in the pre-monsoon and monsoon months of April-June (less than 1.1), which agrees with [18]. This dramatic seasonal shift is the result of fine-mode pollution aerosol hegemony in the winter and post-monsoon months and coarse-mode dust aerosol dominance in the pre-monsoon months. The amount of aerosol loading is observed to be greatest during the winter and pre-monsoon seasons with values surpassing 0.30 and lowest during the summer monsoon season (July and August) with values less than 0.15. Diurnal variations of precipitable water are reported to be minimal throughout the pre-monsoon, winter, and post-monsoon seasons, but the highest diurnal variation of precipitable

water is found during the monsoon season. The seasonality of monsoon precipitation is connected with the strong cycle in total column water vapour, with values reaching 4 cm from June to September. Summer is Lumbini rainy season, accounting for roughly 74% of yearly Precipitation. We observed a substantial adverse connection between visibility and turbidity coefficient (β). Fig. 2(a) illustrates that the values of alpha (α) and beta (β) are nearly opposite during coarse mode particles. Because of particle light extinction, atmospheric visibility is the most intuitive metric of air pollution.

In Pokhara however, we found that the average seasonal Angstrom Exponent was highest in the post-monsoon and winter with values surpassing 1.36, and lowest in the summer monsoon with values less than 1.2. A higher value ($\alpha > 1$) in all seasons implies a columnar aerosol size distribution with a significant contribution from fine mode particles arising mostly from humans, biomass burning, and urban and industrial sources. It shows that aerosol loading is high in March and May with significant fine particles. The seasonal turbidity parameters were highest before the monsoon with values over 0.24 and lowest after the monsoon, with values around 0.06. During the winter and pre-monsoon seasons significant fire spots are found throughout this area increasing the emission of aerosols from biomass burning which flows into Pokhara and affects air quality and increases the Turbidity Coefficient (β) which can reduce visibility. The monthly mean precipitable water vapor exceeds 3.5 cm from June to September accounting for 83% of total annual precipitation. PW rises during the summer monsoon and declines during the post-monsoon season according to seasonal variations. We discovered a significant inverse relationship between visibility and the turbidity coefficient (β). This finding suggests that higher values associated with visibility were related to aerosol loading which was dominated mostly by fine-mode particles.

Furthermore, when compared to Pokhara and Lumbini the annual cycle on monthly mean Angstrom Exponent in Langtang BC is smaller. Fine-mode aerosols dominate the winter, summer-monsoon, and post-monsoon seasons for the majority of the year due to hygroscopic rise and biomass burning (Fig. 2(c)). The highest value of the Angstrom wavelength exponent (α) is larger than 1.07 during the post-monsoon and pre-monsoon seasons, and the minimum value is less than 0.79 during the winter monsoon season (December). The amount of aerosol loading is indicated by the turbidity coefficient (β). The pre-monsoon (April and May) and summer monsoon (August) seasons had the highest aerosol loading with values over 0.0275 while the post-monsoon (October and November) and winter seasons had the lowest with values less than 0.0125. The best visibility was reported to be over 230 km in the post-monsoon and winter seasons and the lowest visibility occurred in the pre-monsoon month of May, with a value of around 170 km. Aerosol loading is lower in Langtang-BC than it is in Pokhara and Lumbini. Because Langtang-BC is located in the Himalayas, it is unaffected by industrial pollutants, vehicular pollution, or other activities. Because biomass burning increases aerosol loading during the pre-monsoon season the populace cooks and heats their homes using traditional fuels such as wood, straw, and dung. These organic fuels cause a high quantity of particles to be released into the atmosphere. The monthly average From June through September, precipitable water vapour surpasses 0.3 cm when 67% of the yearly total precipitation falls. The seasonal fluctuation demonstrates that PW increases during the summer monsoon (July-August) and

decreases throughout the post-monsoon and early pre-monsoon seasons. The winter season had the lowest value of detectable water which was less than 0.1. These findings indicate that the AOD and precipitated water are substantially associated at all locations. As described, much of the removal of atmospheric aerosols happens around big weather systems and high-altitude jet streams, where the stratosphere and lower atmosphere get intertwined and interchange air with each other [17].

IV. Conclusions

For Lumbini monthly averaged AOD (675 nm) showed that the highest and lowest values occurred during the pre-monsoon (0.65) and summer (0.20) respectively but the ranges of AOD in Pokhara and Langtang- BC were lowest. The contribution of pollution particles released from local sources as well as dust particles from long-range transport contributes to the maximum value of AOD (675 nm) in Lumbini during the Pre-monsoon. For Langtang, vegetation burning contributes to spring haze and increases AOD in the pre-monsoon season. As a result of this, AOD at Pokhara and Lumbini were significantly greater than at Langtang each month. The monthly average Angstrom exponent(α) (440-870 nm) in Lumbini ranged from 1.04 to 1.39 with the lowest value occurring in the monsoon season due to frequent dust occurrences. The monthly average Angstrom exponent (440-870 nm) in Pokhara ranged from 1.20 to 1.40. The monthly average Angstrom exponent (440-870 nm) in Langtang-BC ranged from 0.65 to 1.25 with the minimum and maximum values occurring in winter and Post-monsoon. During the post-monsoon household heating activities resulted in the highest values of Angstrom exponent. Precipitation water over Lumbini, Pokhara, and Langtang-BC peaked in summer and lower in the winter season. It is found that visibility and the turbidity coefficient (β) have an inverse relationship. Thus, the turbidity coefficient considerably impacts Visibility. The visibility over Langtang-BC is at the maximum range (170-260 km). Pokhara and Lumbini on the other hand have ranges from 10 to 60 km and 5 to 21 km respectively. In Lumbini, the value of AOD is also higher indicating the possibility of the hygroscopic growth of aerosols and the dust storm from the IGP region. Langtang-BC has the maximum visibility of any other region due to its low population, lack of industrial areas, and its location far from the IGP region.

References

[1] Adam V. Aerosols: tiny particles, big impact. 2020.

[2] Boucher O, Randall D, Artaxo P, Bretherton C, Feingold G, Forster P, et al. Clouds and aerosols. In: Climate change 2013: the physical science basis. Contribution of Working Group I to the Fifth Assessment Report of the Intergovernmental Panel on Climate Change. Cambridge University Press; 2013. p. 571-657.

[3] Ramanathan V, Carmichael G. Global and regional climate changes due to black carbon. Nature geoscience. 2008;1(4):221-7.

[4] Jha R, Adhikari B, Singh D. Study of aerosol optical properties at different tourist places of Nepal. BIBECHANA. 2021;18(1):170-83.

[5] Alam K, Khan R, Ali S, Ajmal M, Khan G, Muhammad W, et al. Variability of aerosol optical depth over Swat in Northern Pakistan based on satellite data. Arabian Journal of Geosciences. 2015;8:547-55.

[6] Richter A, Burrows JP, Nüß H, Granier C, Niemeier U. Increase in tropospheric nitrogen dioxide over China observed from space. Nature. 2005;437(7055):129-32.

[7] Rupakheti D, Kang S, Rupakheti M, Cong Z, Tripathee L, Panday AK, et al. Observation of optical properties and sources of aerosols at Buddha's birthplace, Lumbini, Nepal: environmental implications. Environmental Science and Pollution Research. 2018;25(15):14868-81.

[8] Xu C, Ma Y, Panday A, Cong Z, Yang K, Zhu Z, et al. Similarities and differences of aerosol optical properties between southern and northern sides of the Himalayas. Atmospheric Chemistry and Physics. 2014;14(6):3133-49.

[9] Holben BN, Eck TF, Slutsker Ia, Tanre D, Buis J, Setzer A, et al. AERONET—A federated instrument network and data archive for aerosol characterization. Remote sensing of environment. 1998;66(1):1-16.

[10] Holben BN, Tanre D, Smirnov A, Eck T, Slutsker I, Abuhassan N, et al. An emerging ground-based aerosol climatology: Aerosol optical depth from AERONET. Journal of Geophysical Research: Atmospheres. 2001;106(D11):12067-97.

[11] Wang L, Salazar GA, Gong W, Peng S, Zou L, Lin A. An improved method for estimating the Ångström turbidity coefficient β in Central China during 1961–2010. Energy. 2015;81:67-73.

[12] Seinfeld JH, Pandis SN. From air pollution to climate change. Atmospheric chemistry and physics. 1998;1326.

[13] Tiwari S, Bisht D, Srivastava A, Pipal A, Taneja A, Srivastava M, et al. Variability in atmospheric particulates and meteorological effects on their mass concentrations over Delhi, India. Atmospheric Research. 2014;145:45-56.

[14] Wang B, Shi G. Long-term trends of atmospheric absorbing and scattering optical depths over China region estimated from the routine observation data of surface solar irradiances. Journal of Geophysical Research: Atmospheres. 2010;115(D7).

[15] Ångström A. Techniques of Determinig the Turbidity of the Atmosphere. Tellus. 1961;13(2):214-23.

[16] Iqbal M. An introduction to solar radiation. Elsevier; 2012.

[17] Koschmieder H. Theorie der horizontalen Sichtweite. Beitrage zur Physik der freien Atmosphare. 1924:33-53.

[18] Sapkota S, Gautam S, Pokhrel S, Gautam A, Basnet K, Mishra RK, et al. Study of aerosol optical properties in Lumbini, Nepal. BIBECHANA. 2023;20(1):1-9.